Am J Transl Res 2016;8(12):5659-5671
www.ajtr.org /ISSN:1943-8141/AJTR0028832

Original Article

Identification of chaperones in a MPP$^+$-induced and ATRA/TPA-differentiated SH-SY5Y cell PD model

Hongrong Xie[1*], Hui Hu[1*], Ming Chang[2], Dongya Huang[1], Xiaobo Gu[1], Xinli Xiong[1], Ran Xiong[1], Linsen Hu[2], Gang Li[1]

[1]*Department of Neurology, Shanghai East Hospital, Tongji University, Shanghai 200120,* P. R. *China;* [2]*Department of Neurology, The First Hospital of Jilin University, Shanghai 130021,* P. R. *China.* [*]*Equal contributors.*

Received March 21, 2016; Accepted July 15, 2016; Epub December 15, 2016; Published December 30, 2016

Abstract: Parkinson's disease (PD) is characterized by the pathological accumulation of misfolded proteins. Molecular chaperones assist in the proper folding of proteins and removal of irreversibly misfolded proteins. This study aims to identify potential chaperones associated with protein misfolding and accumulation in PD. ATRA/TPA-differentiated SH-SY5Y cells were treated with 1 mM of MPP$^+$ for 48 hours. Proteins were analyzed by 2D-DIGE followed by MALDI-ToF MS. The treatment of differentiated SH-SY5Y cells by MPP$^+$ led to the unambiguous identification of 10 protein spots, which corresponds to six proteins. Among these six proteins, four were chaperone proteins including nucleophosmin (NPM1), chaperonin-containing TCP-1 subunit 2 (CCT2 or CCTβ), heat shock 90 kDa protein 1 beta (HSP90AB1 or HSP90-β), and tyrosin3/tryptopha5-monoxygenase activation protein, zeta polypeptide (14-3-3ζ, gene symbol: Ywhaz). To our knowledge, this is the first report that linked the upregulation of chaperones after MPP$^+$ treatment with SH-SY5Y cells. However, the NPM1 protein was identified for the first time in the PD model. The upregulation of four chaperone proteins provided evidence that these chaperones have a complementary effect on protein misfolding in the pathogenesis of PD, and hold promise as a good therapeutic target for PD treatment.

Keywords: Chaperone proteins, proteomic analysis, MPP$^+$, SH-SY5Y cells

Introduction

Parkinson's disease (PD) is a progressive neurodegenerative disease caused by the pathological accumulation of misfolded α-synuclein protein. This leads to the formation of intraneuronal inclusion bodies generally referred to as Lewy Bodies (LBs) [1]. It is important for cells to maintain protein homeostasis, and failure to sustain cellular protein homeostasis eventually leads to the accumulation of misfolded proteins and the formation of toxic inclusion bodies. This ultimately results in the induction of cell death. However, due to destabilizing mutations, translation errors and stress conditions, the cell's ability to maintain protein homeostasis is constantly challenged [2]. Recent evidence has suggested that α-synuclein assembly is one of the first steps in the degenerative process of PD [3], and oligomeric intermediates are indeed toxic, specifically to neurons [4]. Therefore, preferred therapeutic approaches for PD should aim in preventing the early steps of oligomerization and aggregation, in order to halt the degenerative process caused by protein misfolding and accumulation. In fact, human cells have adopted an elaborate protein quality-control system to maintain intracellular protein homeostasis, which involve a highly conserved network of molecular chaperones [5]. Molecular chaperones not only assist in the proper folding and refolding of proteins in a crowded cellular environment [6], but also effectively remove irreversibly misfolded proteins through protein degradation pathways such as the ubiquitin-proteasome system (UPS) and the autophagy-lysosomal pathway [7]. Interestingly, growing evidence suggests that chaperones are capable of preventing α-synuclein misfolding, oligomerization and aggregate formation *in vitro* and in animal models of PD [8]. Therefore, in order to specifically identify potential chaperones associated with protein misfolding and accumulation in PD, we investi-

gated proteomic changes in SH-SY5Y cells treated with all-trans-retinoic acid and phorbol ester 12-O-tetradecanoylphorbol-13-acetate (ATRA/TPA), followed by 1-methyl-4-phenyl-pyridinium ion (MPP^+) treatment *via* two-dimensional difference ingel electrophoresis (2D-DIGE) and matrix-assisted laser desorption/ionization time-of-flight mass spectrometry (MALDI-ToF MS). This model has been widely used to study various aspects of the neurodegenerative process associated with idiopathic PD. The clear understanding of molecular chaperones related to protein folding would ultimately facilitate the elucidation of PD pathogenesis. Furthermore, this holds promise as an alternate therapeutic target for PD.

Materials and methods

Chemicals

All reagents used in this study were of analytical grade and of the highest purity. Dulbecco's modified Eagle's medium (DMEM) and fetal bovine serum (FBS) were purchased from Gibco (Grand Island, NY, USA). N,N,N',N'-tetramethylethylenediamine (TEMED) was procured from Promega (Madison, WI, USA). Urea, sodium dodecyl sulphate (SDS), glycine, Tris (hydroxymethyl) aminomethane (Tris), bromophenol blue, ammonium persulfate, trypsin (sequencing grade), α-cyano-4-hydroxycinnamic acid (α-HCCA), trifluoroacetic acid (TFA), dithiothreitol (DTT), acrylamide, methylenebisacrylamide, 3-[(3-cholamidopropyl) dimethyl-ammonio]-1-propane sulfonate (CHAPS), thiourea, iodoacetamide, Clean-up kit, 2D-Quant kit, nuclease mix, PhastGel Blue R250 tablets, immobilized pH-gradient (IPG) strip (pH 4-7), IPG buffer (pH 4-7), and fluorescent dyes Cy2, Cy3 and Cy5 were all obtained from Amersham Biosciences-GE Healthcare (Uppsala, Sweden). The remaining other chemicals were obtained from Sigma-Aldrich, unless otherwise stated.

Cell culture, differentiation and MPP^+ treatment

Human dopaminergic SH-SY5Y cells (American Type Culture Collection; ATCC, Rockville, MD) were grown in high-glucose DMEM supplemented with 5% fetal bovine serum, 60 μg/ml of penicillin and 100 μg/ml of streptomycin; and incubated at 37°C under a saturating humidified atmosphere of 5% CO_2. The procedure for generating a fully differentiated dopaminergic neuronal phenotype of SH-SY5Y cells was carried out according to a previously published report [9]. Briefly, cells were plated at an initial density of 1×10^4 cells/ml. Then, cells were differentiated by exposure to medium containing 10 mM of ATRA for three days; and the media was removed and replaced with fresh 80 nM of TPA medium for another three days. Stock solutions of ATRA and TPA were dissolved in DMSO, stored at -20°C in the dark, and diluted in culture medium. The final concentration of DMSO in the medium was not allowed to exceed 0.1%. Finally, the differentiated cells were treated with freshly prepared MPP^+ (1 mM) for 48 hours. Terminally differentiated SH-SY5Y cells without MPP^+ treatment were used as control.

MTT assay

Cell viability was detected by 3-(4,5-dimethylthiazol-2-yl)-2,5-diphenyltetrazolium bromide (MTT) assay. Differentiated cells were treated with MPP^+ for 48 hours, and incubated with 10 μl of MTT solution (5 mg/ml in PBS) for four hours at 37°C. Then, 100 μl of DMSO was added to dissolve the formazan precipitate; and absorbance was measured at 570 nm using a 96-well ELISA microplate reader (Bio-Rad Model 680, Hercules, CA, USA). The control cells were also treated in the same condition. Each treatment was performed in five wells, and every experiment was independently repeated three times.

Trypan blue exclusion

SH-SY5Y cells were cultured and differentiated in 96-well culture plates. After treatment with 1 mM of MPP^+ for 48 hours, cells were stained with trypan blue dye (final concentration of 0.67%) for two minutes. Viable (non-colored) and dead (blue-colored) cells were counted under an inverse phase microscope (Olympus, Tokyo, Japan) at 400× magnification. Cell death rate was analyzed as the ratio of dead cells to the total cells.

Hoechst 33342 staining

Differentiated cells treated with 1 mM of MPP^+ were incubated for 48 hours with 0.1 mg/ml of Hoechst 33342 dye for 30 minutes at 37°C. Nuclear morphological changes were observed under a fluorescence microscope (Olympus,

Tokyo, Japan). The control SH-SY5Y cell nuclei displayed a regular and ovum shape. As identified by their characteristic nuclei condensation, cell fragmentation and cells that appeared bright were considered as apoptotic cells. For each experiment, at least 300 cells were counted from more than five random microscopic fields, in order to calculate the percentage of apoptotic cells. The experiment was repeated three times.

Protein sample preparation

Terminally differentiated SH-SY5Y cells with or without MPP^+ treatment were harvested and washed with sucrose buffer (10 mM of Tris, 250 mM of sucrose, pH 8.0). Then, treated cells were lysed with lysis buffer containing 7 M of urea, 2 M of thiourea, 4% CHAPS, 30 mM of Tris and a 1% protease inhibitor cocktail with a nuclease mix for one hour at room temperature. After centrifugation (25,000×g for 30 minutes at 15°C), the supernatants were collected, cleaned with a Clean-up kit, and subsequently quantified using a 2D-Quant kit following manufacturer's instructions. For 2D-DIGE, four independent extractions were performed from MPP^+-treated and -differentiated SH-SY5Y and control cells. Samples were stored at -80°C for further analysis.

2D-DIGE and image analysis

In order to perform the 2D-DIGE analysis, samples were pre-labeled with one of the three CyFluor dyes (Cy2, Cy3 and Cy5), each with a unique fluorescent wavelength. Each fluorescent dye can be separated on the same 2D gel. The pH of the samples was adjusted to 8.5 to optimize fluorescent labeling. Half of the samples from each group were labeled with Cy3, and another half were labeled with Cy5 to avoid any possible bias derived from dye labeling. The internal standard, which is a pool of equal amounts of all experimental samples, were labeled with Cy2. After pre-labeling, 50 μg of Cy3- and Cy5-labeled experimental samples and 50 μg of Cy2-labeled internal standard were combined and diluted with 450 μl of rehydration buffer (7 M of urea, 2 M of thiourea, 2% CHAPS, 0.4% IPG buffer, 0.28% DTT, and 0.4% bromophenol blue) to have equal volumes. Isoelectric focusing (IEF) was carried out on an IPGphor system (Amersham Biosciences-GE Healthcare, Uppsala, Sweden) using 24-cm IPG gel strips (pH 4-7) at 20°C under the following conditions: six hours at 0 V for passive rehydration, six hours at 30 V for active rehydration, three hours at 500 V, one hour each at gradients of 1,000 V and 8,000 V, and finally, seven hours at 8,000 V. Focused IPG strips were reduced for 15 minutes in equilibration buffer I (50 mM of Tris pH 8.8, 6 M of urea, 30% glycerol, 2% SDS, 0.2% bromophenol blue, and 1% DTT) and alkylated for 15 minutes in equilibration buffer II (buffer II was identical to buffer I, but with 2.5% iodoacetamide instead of DTT). Then, two-dimensional separations were performed on homogenous 12.5% polyacrylamide gels using an Ettan DALT Six system (Amersham Biosciences-GE Healthcare, Uppsala, Sweden) at 2 W/gel until the bromophenol blue dye front reached the lower end of the gels. DIGE gels were scanned with a Typhoon 9400 laser scanner (Amersham Biosciences-GE Healthcare, Uppsala, Sweden) at a resolution of 100 μm in three different wavelengths to obtain individual images of the Cy2, Cy3 and Cy5 components of each gel. Gel analysis was carried out using the DeCyder Differential In-gel Analysis software (Amersham Biosciences-GE Healthcare, Uppsala, Sweden) to co-detect and quantify protein spots in images according to the protocols provided by the manufacturer.

In-gel digestion and MALDI-ToF MS analysis

MALDI-ToF-MS analysis was conducted according to the previously published method by our lab [10]. In order to identify individual spot proteins from the 2D-DIGE analysis, the preparative gels of samples from MPP^+-treated and -differentiated SH-SY5Y cells and controls were prepared with 600 μg of protein in the same conditions as above. Next, the preparative gels were fixed in 20% TCA for one hour followed by Coomassie bright blue staining. Spots of interest were excised using an Ettan Spot Picker (Amersham Biosciences-GE Healthcare, Uppsala, Sweden), destained by washing with 0.4% ammonium bicarbonate in 50% methanol twice, and dehydrated in 100% acetonitrile (ACN) for one hour. After desiccation, proteins were digested with trypsin solution (20 μg/μl of trypsin in 20 mM of ammonium bicarbonate) overnight at room temperature. Digestion was stopped by adding 1% TFA in 50% ACN. Then, proteolytic peptides were transferred into new 96-well plates, dried completely, and redis-

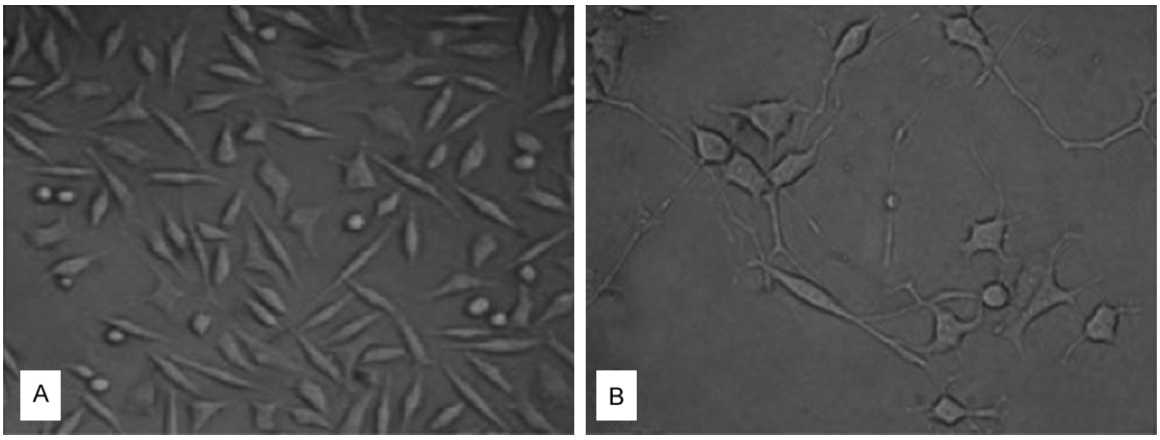

Figure 1. Morphological changes induced by the ATRA/TPA differentiation of SH-SY5Y cells are shown. A. Shows the morphology of undifferentiated SH-SY5Y cells cultured for six days. B. Shows the morphology of SH-SY5Y cells differentiated with 10 uM of ATRA for three days followed by 80 nM of TPA treatment for another three days. All images were captured under an inverted phase contrast microscope with 200× magnification.

solved in 50% ACN/0.1% TFA solution. Finally, the samples were mixed with a matrix (4 mg/ml of α-HCCA in 50% ACN/0.1% TFA) and spotted onto MALDI-ToF MS target slides by an Ettan Spotter (Amersham Biosciences-GE Healthcare, Uppsala, Sweden).

Peptide mass fingerprints (PMFs) were obtained by MALDI-ToF MS (Amersham Biosciences-GE Healthcare, Uppsala, Sweden) operated in the positive ion reflection mode, with trypsin autodigestion peaks as the internal calibration and hACTH (19-39) and Ang III as the external calibration. Accelerating voltage was set at 20 kV with a laser mode of 200 shots for each spectrum. PMFs were searched against the National Center for Biotechnology Information (NCBI) database with the help of the ProFound search engine (fully integrated into the Ettan MALDI-ToF system or at www.ncbi.nlm.nih.gov) for initial identification. The basic criteria for identification was an expectation value (chance of misidentification) ≤0.05 and a coverage (the ratio of the protein sequence covered by matched peptides) ≥20%. Initial identifications were further confirmed by searching in the SWISS-PROT protein sequence database (http://au.expasy.org/sprot/) with Mascot.

Statistical analysis

All data were expressed as mean ± standard deviation (SD). Comparisons were made using ANOVA and Student's *t*-test between the two groups. Statistical significance was defined as $P<0.05$.

Results

Morphological characteristics of differentiated SH-SY5Y cells

SH-SY5Y cells were differentiated by treatment with 10 mM of ATRA for three days followed by additional treatment with 80 nM of TPA for another three days. These differentiated cells displayed dramatic morphological changes during the six-day treatment. It appeared that these differentiated SH-SY5Y cells stopped replicating to a stable population and revealed numerous elongated processes, while undifferentiated SH-SY5Y cells proliferated continuously and had a basal neuroblast-like morphology with rounded cell bodies and few or no short processes, as shown in **Figure 1**. This observation was consistent with a previously published study [9]. In addition, ATRA/TPA-differentiated SH-SY5Y cells closely resembled *in vivo* dopaminergic neurons compared with undifferentiated cells.

Effect of MPP+ on the cell viability of differentiated SH-SY5Y cells

Since MPP+ treatment has been widely used to induce certain aspects of the neurodegenerative process associated with idiopathic PD, the cytotoxic effect of MPP+ on ATRA/TPA-differentiated SH-SY5Y cells was first examined using mitochondrial activity-dependent MTT assay. Our data revealed that cell viability decreased to 54.3% ± 0.8% after treatment with MPP+ (1.0 mM) for 48 hours. The optimum

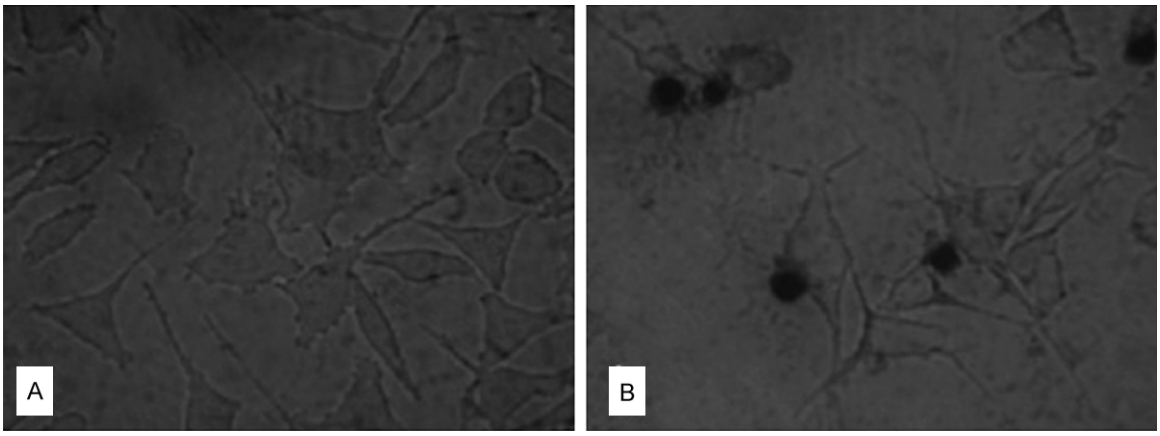

Figure 2. Analysis of MPP+-induced cell death. A. Shows the trypan blue staining of SH-SY5Y cells treated with the vehicle. B. Shows the trypan blue staining of SH-SY5Y cells treated with 1 mM of MPP+ for 48 hours. Pictures were recorded at 400× magnification.

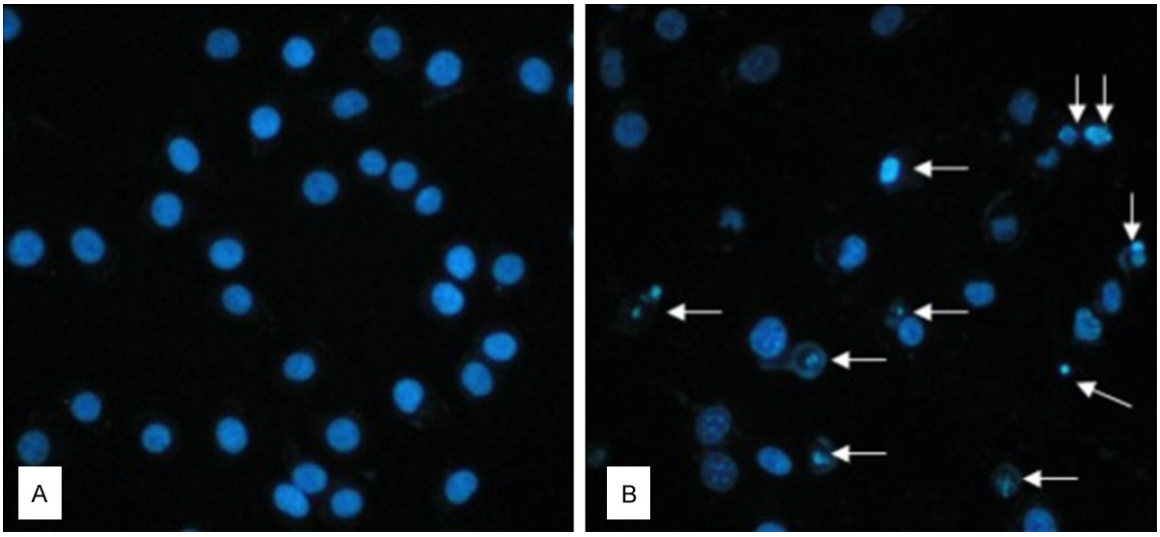

Figure 3. Assessment of the nuclear morphological changes of MPP+-treated SH-SY5Y cells. Fluorescence micrographs show SH-SY5Y nuclei staining with Hoechst 33342. A. Cells treated with the vehicle. B. Cells treated with 1.0 mM of MPP+ for 48 hours. Arrows indicate the nuclei of apoptotic cells. Pictures were recorded at 200× magnification.

concentration of MPP+ used in our experiments was determined by preliminary experiments (data not shown).

Next, the induction of cell death was analyzed by Trypan blue exclusion assay. It appears that MPP+ treatment did result in the induction of cell death, since there was an apparent increase in dead cells, which was stained blue after MPP+ exposure. Treatment with 1 mM of MPP+ for 48 hours revealed a 38.3 ± 2.1% rate of cell death, as shown in **Figure 2**. Apoptosis at post MPP+ treatment was also determined by the Hoechst 33342 staining method. The exposure of 1.0 mM of MPP+ for 48 hours induced a 35.3 ± 1.5% apoptotic cell death, as shown in **Figure 3**.

These data revealed that there was a partial induction of apoptosis on one hand and a simultaneous reduction in cell viability on the other. However, overall, approximately 50% of MPP+-treated SH-SY5Y cells remained alive. This could be attributed to the fact that MPP+-induced toxicity/stress led to protein misfolding, aggregation and the induction of cell apop-

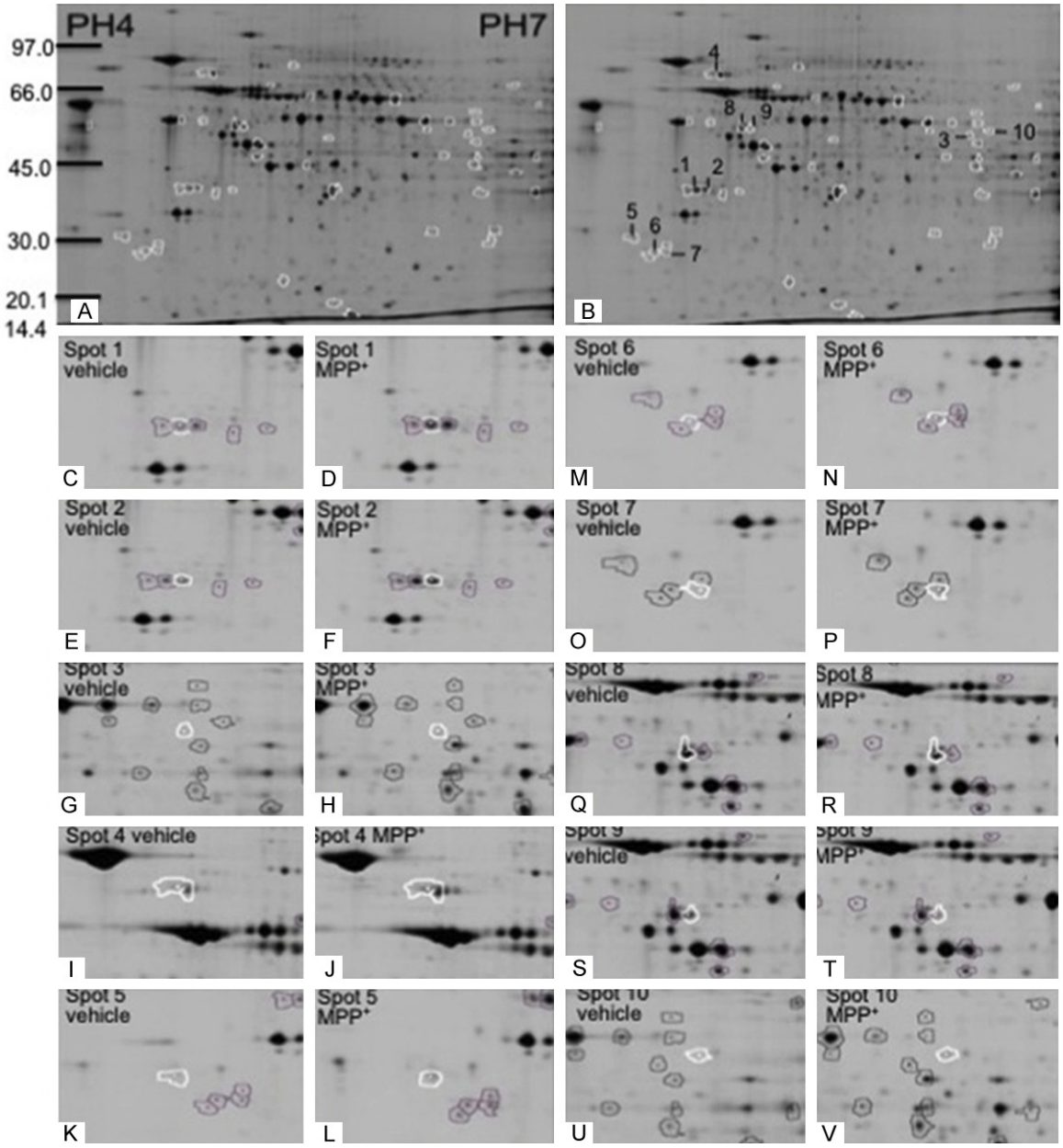

Figure 4. Representative 2D-DIGE gel images showing protein expression changes in SH-SY5Y cells with or without MPP+ treatment is shown. Protein spots in 2D-DIGE gels were analyzed using DeCyder software, and spots-of-interest with greater than 1.3-fold changes between SH-SY5Y cells with and without MPP+ treatment were marked with white circles. (A) Depicts the image of protein spots from vehicle-treated cells labeled with Cy3. (B) Depicts the image of protein spots from MPP+-treated cells labeled with Cy5. The identity of proteins in the spots was determined by MALDI-ToF MS, and the identified spots were marked with numbers in image (B). Spot numbers in this figure correspond to those listed in **Tables 1** and **2**. Panels (C to V) depicts the more detailed information on the spots-of-interest from 2D-DIGE by DeCyder software (spot 1 [C-D], spot 2 [E-F], spot 3 [G-H], spot 4 [I-J], spot 5 [K-L], spot 6 [M-N], spot 7 [O-P], spot 8 [Q-R], spot 9 [S-T], and spot 10 [U-V]). Panels (C, E, G, I, K, M, O, Q, S and U) display partial images of protein spots in the 2D-DIGE gel from vehicle-treated cells, where panel (D, F, H, J, L, N, P, R, T and V) shows corresponding partial images in the 2D-DIGE gel from MPP+-treated cells. There are more than one spot identified as the same protein such as nucleophosmin (spots 1 and 2), 14-3-3ζ (spots 5, 6 and 7), and α-tubulin (spots 8 and 9); which may represent some PTMs.

tosis. Furthermore, this may have also simultaneously upregulated the expression of some neuroprotective proteins such as chaperones to restore protein homeostasis. Thus, this

Table 1. List of proteins identified though MALDI-ToF MS analysis

Spot no.	Protein name	NCBI accession number	Theoretical values		Sequence coverage %	Expectation
			Mr	pI		
Chaperone protein						
1	Nucleophosmin/B23.2	Gil13536991	23.6	4.6	23.6	0.006
2	Nucleophosmin/B23.2	Gil13536991	23.9	4.6	23.9	0.027
3	Chaperonin containing TCP 1 subunit 2	Gil543603	57.81	6.0	29.9	0.000
4	Heat shock 90 kDa protein 1, beta	Gil20149594	83.59	5.0	23.9	0.000
5	14-3-3ζ	Gil5803225	29.33	4.6	35.3	0.001
6	14-3-3ζ	Gil49119653	30.1	4.7	34.0	0.000
7	14-3-3ζ	Gil4507949	28.18	4.8	24.0	0.002
Cytoskeleton						
8	α-tubulin	Gil4389309	50.56	5.0	31.0	0.000
9	α-tubulin	Gil57013276	50.82	4.9	32.6	0.000
Serine biosythesis						
10	3-phosphoglycerate dehydrogenase	Gil5771523	57.39	6.3	22.0	0.000

Mr: indicates molecular weight; pI: isoelectric point; 14-3-3ζ: tyrosin3-monooxygenase/tryptophan5-monooxygenase activation protein, zeta polypeptide; Expectation: chance of incorrect identification.

Table 2. Fold changes of identified proteinsafter MPP treatment

Spot no.	Protein	Fold change in protein expression (MPP+-treated SH-SY5Y cells/controls)	*P* value student's t-test
1	Nucleophosmin	2.16	1.2e-006
2	Nucleophosmin	2.06	1.4e-005
3	Chaperonin containing TCP-1 subunit 2	1.70	0.015
4	Heat shock 90 kDa protein 1 beta	1.93	3.6e-006
5	14-3-3ζ	1.36	0.00099
6	14-3-3ζ	1.47	0.00024
7	14-3-3ζ	1.99	1.3e-006
8	α-tubulin	-1.67	0.00039
9	α-tubulin	-1.46	0.014
10	3-phosphoglycerate dehydrogenase	1.95	0.012

14-3-3ζ: tyrosin3-monooxygenase/tryptophan5-monooxygenase activation protein, zeta polypeptide.

resulted in the survival of some cells. Therefore, the specific analysis of elevated proteins in the cell population that survived could shed some light on the role played by MPP+ treatment.

2D-DIGE analysis of proteins in differentiated SH-SY5Y cells with or without MPP+ treatment

In order to identify chaperone proteins with expression levels manipulated as a result of the MPP+ treatment of differentiated SH-SY5Y cells, a 2D-DIGE analysis was performed, as described in the Materials and Methods section. 2D-DIGE fluorescent gel images were analyzed with the DeCyder software, which provided spot detection, spot matching and quantitative values. The use of the internal standard and three CyDye Fluor dyes (Cy2, Cy3 and Cy5) effectively helped to normalize data among the gels. This led to the accurate estimation of data, along with increased statistical confidence by quantitative comparative analysis; which eliminated most of the technical variations. Proteins that were detected in at least three gels out of four were further considered for quantitative analysis. Protein spots with a ≥1.3-fold expression change and statistical significance ($P<0.05$) estimated by student's *t*-test were defined as differentially expressed proteins. Based in this criterion, a total of 49 protein spots were further analyzed on MALDI-ToF MS, as shown in **Figure 4**.

The identification of proteins affected by MPP+ treatment

Finally, in order to identify these differentially expressed proteins, the spots-of-interest were excised from Coomassie brilliant blue-stained preparative gels, and digested with trypsin for analysis by MALDI-ToF MS. Among the 49 spots-of-interest identified by 2D-DIGE analysis, 10 protein spots were further analyzed successfully by MALDI-ToF MS using an in-house licensed ProFound search engine and by searching the NCBI protein database restricted to *Homo sapiens*. The criteria for the positive identification of proteins with MS were set as an expectation ≤0.05 and a coverage ≥20%. The matching of molecular weight and the isoelectric point to those derived from the spot position on the gels provided additional verification for the identification. **Table 1** lists the detailed information of identified proteins assessed by the NCBI protein database. Protein expression changes of these proteins are described in **Table 2**. In some cases, more than one protein spot corresponded with the same protein, which might represent different post-translational modifications (PTMs) of the same protein; leading to the minor drift of molecular weight and pI. Finally, eight proteins were actually identified. Interestingly, different PTMs of the same protein expressed a similar fold change. Except for tubulin (resolved as two distinct spots) and 3-phosphoglycerate dehydrogenase (Phgdh), all other proteins were molecular chaperones upregulated by MPP+ treatment, including nucleophosmin (NPM1, resolved as two distinct spots), chaperon-containing TCP-1 subunit 2 (CCT2 or CCTβ), heat shock 90 kDa protein 1 beta (HSP90AB1 or HSP90β), and tyrosin3/tryptopha5-monoxygenase activation protein, zeta polypeptide (YWHAZ or 14-3-3ζ, three distinct spots were identified as YWHAZ). All these data are shown in **Table 1** and **Figure 4**. These proteins were further verified by searching the SWISS-PROT protein sequence database.

Discussion

Chaperones are a class of proteins that interact, stabilize and help other proteins to acquire their native conformation, and are implicated in the regulation of protein misfolding and aggregation process in cells [11]. Many previous studies have focused on the neuroprotective role of chaperone proteins in PD, which is defined as conformational disorder characterized by misfolding, aggregation and Lewy Body formation. In this study, we identified the upregulation of four chaperone proteins in the protein profile of MPP+-treated SH-SY5Y cells, which included NPM1, chaperonin-containing TCP-1 subunit 2 (CCT 2 or CCTβ), heat shock 90 kDa protein 1 beta (HSP90AB1 or HSP90-β), and tyrosin3/tryptopha5-monoxygenase activation protein, zeta polypeptide (14-3-3ζ, gene symbol Ywhaz). In addition, some of these chaperone proteins have been previously been reported to be associated with the pathogenesis of PD. To our knowledge, this is the first report that linked the upregulation of these chaperone proteins to MPP+ treatment. Furthermore, this study reports for the first time that NPM1 protein is involved in PD. The upregulation of these chaperones can be explained as a defensive mechanism to combat the increased misfolding of certain proteins or in response to the induction of apoptosis in the MPP+-induced SH-SY5Y cell PD model. These might prove to be potential targets for further therapeutic studies of PD.

Nucleophosmin (NPM1, also known as B23, NO38, or numatrin)

NPM1, also called nucleolar protein B23, numatrin, or NO38, is a member of the nucleoplasmin family of histone chaperones, which is involved in mediating DNA-histone and nucleosome assembly [12]. In addition to its specific role as a histone chaperone, NPM1 also functions as a broad molecular chaperone on a wide variety of substrates, including interacting with a wide range of unfolded proteins. This induces proper folding in the active state, inhibits protein aggregation, and promoting the renaturation of chemically denatured proteins [13, 14]. The upregulation of NPM1 in the present study might be involved in the neuroprotective effects of the MPP+-induced PD cell model. Through its molecular chaperone function, the aggregation and misfolding of proteins can be attenuated in the pathogenesis of PD. In addition to its role as a chaperone, NPM1 is a multifunctional protein that has been shown to play an important role in many other cellular activities including cell growth, proliferation and apoptosis [15]. Hence, the potential protective

role played by the overexpression of NPM1 in the present study can also be linked to its anti-apoptotic function [16]. NPM1 has been shown to be involved in the stabilization of tumor suppressor protein p53 [17], and function as a BCL2-associated X protein (BAX) chaperone [18] and a cytoplasmic/nuclear shuttle protein [19]; which limit apoptosis. NPM1 is highly expressed in the brain, but its function in post-mitotic neurons remains obscure. Furthermore, several studies have recently found that NPM1 is involved in neurodegenerative diseases [20]. The exact mechanism of the contribution of NPM1 in PD remains completely unelucidated, and it is unclear whether it functions as a molecular chaperone or an anti-apoptotic protein. Thus, the possible link between NPM1 and PD should be seriously considered in future studies.

Chaperonin containing t-complex polypeptide 1 (TCP1), subunit 2 (beta) (CCT2 or CCTβ)

Chaperonin-containing TCP-1 (CCT), also called TCP-1 Ring complex (TRiC) or C-cpn, essentially has a chaperone function that contributes to cellular protein homeostasis by assisting in *de novo* folding, preventing protein aggregation and degrading many denatured proteins in eukaryotic cells [21]. TRiC/CCT has specific structural and mechanistic features that fold some of the essential substrate proteins, in which some of these proteins could not be folded by other chaperone systems such as cytoskeletal components and cell cycle regulators [22]. TRiC/CCT CCT is the most complex of all the chaperones, with each of the two rings composed of eight distinct and paralogous subunits [23] of approximately 60 kDa molecular weight, which are named α, β, γ, δ, ε, ζ, η and θ in mammalian cells (CCT1-8 in yeast) [24]. Although the CCT oligomer is essential for folding activities, increasing evidence suggests that CCT monomers themselves can function, independent of the TRiC/CCT complex [25]. In the present study, individual CCT2 levels were upregulated in MPP+-treated SH-SY5Y cells, implicating that CCT2 might play a role in the protein-folding machinery of PD pathogenesis. Therefore, it is hypothesized that the enhancement of CCT2 levels may facilitate delaying or preventing the development of MPP+-induced PD. In addition, as a predominant molecular chaperone of cytoskeletal proteins, the upregulation of CCT2 during exposure to MPP+ might be a response to cytoskeleton abnormality, which is common in PD [26, 27]. The alteration of α-tubulin protein in the present study might also partially result into the upregulation of CCT, because CCT can regulate the level of tubulin *via* a direct *de novo* synthesis or rapid degradation of non-native tubulin [25]. Our results suggest that CCT2 might play an essential role in the modulation of protein folding, which could be another target for further therapeutic studies of PD.

Heat shock protein 90AB1 (HSP90AB1 or HSP90 β)

HSP90 has been recently identified as the predominant chaperone implicated in α-synuclein-evoked PD pathologies [28, 29], which is capable of preventing α-synuclein misfolding, oligomerization and aggregation; thus, suppressing α-synuclein misfolding-induced PD toxicity [30]. HSP90 has two cytosolic isoforms, HSP90-α and HSP90-β; which are 85% identical. The upregulation of HSP90-β in this study was consistent with previous findings, in which HSP90 levels increased under oxidative stress in cell cultures [31], 6-OHDA-lesioned rats [32], and human PD brains [33]. These current results might represent the neuroprotective role of HSP90-β as a chaperone in MPP+-induced PD mimicking. However, HSP90 can also assist in the stability of some aberrant neuronal proteins; and thus, result in the formation of toxic aggregates [34, 35]. It has been found that HSP90 is implicated in the negative regulation of heat shock factor-1 (HSF-1), which is a master transcriptional regulator of HSPs. Thus, the HSP90 inhibitor might activate HSF-1 to induce the overexpression of HSP70, HSP40 and other chaperones that in turn reduce neurodegeneration by refolding and solubilizing aberrant proteins [36]. Some experimental findings have proven that HSP90 inhibitors can suppress neurodegeneration and exhibit protective effects in the PD model [37, 38]. In the review of Luo W *et al.*, HSP90 inhibitors have been proposed as a potential beneficial therapy in neurodegenerative diseases including PD [39]. Recent reviews have suggested that a number of small molecular inhibitors of HSP90 can decrease α-synuclein oligomerization *in vitro* and rescue α-synuclein-induced toxicity in PD models [40]. However, their utility is limited

due to high toxicity, brain permeability, and drug design [41]. Therefore, the result of our study provides an updated view of the role of HSP90 in PD; suggesting that it might become a promising clinical therapeutic agent against the neurodegenerative progression of PD in the future.

Tyrosine 3-monooxygenase/tryptophan 5-monooxygenase activation protein, zeta polypeptide (YWHAZ or 14-3-3ζ)

YWHAZ or 14-3-3 zeta (14-3-3ζ) is a member of the ubiquitous cytoplasmic chaperone protein family 14-3-3 [42], which include seven separate gene or isoform coding sequences for these proteins in mammals (denoted by Greek letters: β, γ, ε, ζ, η, τ and δ) [43]. Our study demonstrated that 14-3-3ζ was upregulated in the PD cellular mimicking model, which is consistent with previous reports that implicated 14-3-3 proteins in the pathogenesis of PD [44, 45]. Since, 14-3-3ζ has been shown to co-localize with α-synuclein in LBs in human PD [46], the overexpression of 14-3-3ζ in our study may have resulted from elevated α-synuclein levels. Intriguingly, 14-3-3ζ has been shown to dissolve aggregated proteins and eliminate misfolded proteins [47]; thus, leading to the hypothesis that its accumulation in LBs may be particularly beneficial to DA neurons in PD. In addition, 14-3-3 proteins appears to be a key interacting partner of leucine-rich repeat protein kinase 2 (LRRK2); and its mutation is the most common cause of familial PD. Several PD-associated LRRK2 mutants have been shown to decrease the interaction of 14-3-3 proteins [48, 49]. Except for α-synuclein and LRRK2, 14-3-3 proteins have also been shown to interact with Parkin, which is another PD gene [50]. Thus, it is reasonable to believe that indeed 14-3-3 proteins might be associated with the pathogenesis of PD, because 14-3-3 proteins did interact with LRRK2, α-synuclein and parkin genes; in which its mutations can cause PD in a dominant fashion. Furthermore, 14-3-3ζ can activate tyrosine hydroxylase (TH), a rate-limiting enzyme in the biosynthesis of dopamine; while wild-type α-synuclein can inhibit TH and DA synthesis in a dose-dependent manner [51]. Thus, the upregulation of 14-3-3ζ may act as a cellular compensation of α-synuclein toxicity for restoring the reduction of dopamine in the pathogenesis of PD [52]. The protective role of 14-3-3 proteins was also supported by another report, which suggested that the pharmacological inhibition of 14-3-3 proteins can enhance neurotoxic vulnerability, whereas 14-3-3 overexpression has a protective effect in the transgenic *C. elegans* model of PD [53]. In addition to its own intrinsic chaperone-like activity, 14-3-3 proteins can also inhibit apoptosis; because they can lead to the suppression of the pro-apoptotic function and activation of anti-apoptotic proteins [54-56]. Thus, the contribution of 14-3-3ζ to the pathogenesis of PD might be due to its chaperone function, which binds proteins involved in dopaminergic degeneration and apoptosis, such as α-synuclein, LRRK2, apoptosis signal-regulating kinase 1 (ASK1) [57], Bcl-2 family protein BAD [58], Bcl-2 [59], Bcl2-associated X protein (Bax) [60], caspase-2 [61], and Fkhrl1 (a member of the family of Forkhead transcription factors) [62]. Moreover, 14-3-3ζ may also exert its protective role *via* maintaining calcium homeostasis [63]. Undoubtedly, the 14-3-3 protein is crucial to PD pathogenesis; and the overexpression of 14-3-3ζ in this study suggests its protective mechanism, which is a potential therapeutic target for PD.

Conclusion

Taken together, our data demonstrates that several chaperone proteins were closely related with neurotoxicity in a MPP+-induced PD cellular model. This indicates that the upregulation of various chaperones might be required to prevent the misfolding and aggregation of harmful proteins, and protect dopaminergic neurons in the pathogenesis of PD. Due to the increased incidence of PD patients in our aging society, there is an urgent need to find effective therapeutic approaches to this devastating disease. Chaperones might hold the promise to open the therapeutic door for PD patients by reversing the misfolding and neurodegeneration of harmful proteins.

Acknowledgements

This work was supported by the Distinguished Professor Foundation of Jilin University to Dr. Linsen Hu (450011011204).

Disclosure of conflict of interest

None.

Address correspondence to: Dr. Linsen Hu, Department of Neurology, The First Hospital of Jilin University, 71 Xinmin Street, Changchun 130021, P. R. China. Tel: +86-431-85674320; Fax: +86-431-56-37090; E-mail: hulinsen@hotmail.com; Dr. Gang Li, Department of Neurology, Shanghai East Hospital, Tongji University, 1800 Yuntai Road, Shanghai 20-0123, P. R. China. Tel: +86-13621691786; E-mail: ligang@tongji.edu.cn

References

[1] Ciechanover A, Kwon YT. Degradation of misfolded proteins in neurodegenerative diseases: therapeutic targets and strategies. Exp Mol Med 2015; 47: e147.

[2] Shiber A, Ravid T. Chaperoning Proteins for Destruction: Diverse Roles of Hsp70 Chaperones and their Co-Chaperones in Targeting Misfolded Proteins to the Proteasome. Biomolecules 2014; 4: 704-724.

[3] Chaari A, Hoarau-Véchot J, Ladjimi M. Applying chaperones to protein-misfolding disorders: Molecular chaperones againstα-synuclein in Parkinson's disease. Int J Biol Macromol 2013; 60: 196-205.

[4] Ebrahimi-Fakhari D, Wahlster L, McLean PJ. Molecular Chaperones in Parkinson's Disease - Present and Future. J Parkinsons Dis 2011; 1: 299-320.

[5] Jia B, Wu Y, Zhou Y. 14-3-3 and aggresome formation: Implications in neurodegenerative diseases. Prion 2014; 8: 173-177.

[6] Hetz C, Mollereau B. Disturbance of endoplasmic reticulum proteostasis in neurodegenerative diseases. Nat Rev Neurosci 2014; 15: 233-249.

[7] Brodsky JL. The threads that tie protein-folding diseases. Dis Model Mech 2014; 7: 3-4.

[8] Dimant H, Ebrahimi-Fakhari D, McLean PJ. Chaperones and Co-Chaperones in Parkinson Disease. Neuroscientist 2012; 18: 589-601.

[9] Presgraves SP, Ahmed T, Borwege S, Joyce JN. Terminally differentiated SH-SY5Y cells provide a model system for studying neuroprotective effects of dopamine agonists. Neurotox Res 2004: 5: 579-598.

[10] Xie H, Chang M, Hu X, Wang D, Tian M, Li G, Jiang H, Wang Y, Dong Z, Zhang Y, Hu L. Proteomics analysis of MPP+-induced apoptosis in SH-SY5Y cells. Neurol Sci 2011; 32: 221-228.

[11] Ebrahimi-Fakhari D, Saidi LJ, Wahlster L. Molecular chaperones and protein folding as therapeutic targets in Parkinson's disease and other synucleinopathies. Acta Neuropathol Commun 2013; 1: 79.

[12] Arnoldo L, Sgarra R, Chiefari E, Iiritano S, Arcidiacono B, Pegoraro S, Pellarin I, Brunetti A, Manfioletti G. A novel mechanism of post-translational modulation of HMGA functions by the histone chaperone nucleophosmin. Sci Rep 2015; 5: 8552.

[13] Leal MF, Mazzotti TK, Calcagno DQ, Cirilo PD, Martinez MC, Demachki S, Assumpção PP, Chammas R, Burbano RR, Smith MC. Deregulated expression of Nucleophosmin 1 ingastric cancer and its clinicopathological implications. BMC Gastroenterol 2014; 14: 9.

[14] Colombo E, Alcalay M, Pelicci PG. Nucleophosmin and its complex network: a possible therapeutic target in hematological diseases. Oncogene 2011; 30: 2595-2609.

[15] Mitrea DM, Grace CR, Buljan M, Yun MK, Pytel NJ, Satumba J, Nourse A, Park CG, Madan Babu M, White SW, Kriwacki RW. Structural polymorphism in the N-terminal oligomerization domain of NPM1. Proc Natl Acad Sci U S A 2014; 111: 4466-4471.

[16] Qing Y, Yingmao G, Lujun B, Shaoling L. Role of Npm1 in proliferation, apoptosis and differentiation of neural stem cells. J Neurol Sci 2008; 266: 131-137.

[17] Wong JC, Hasan MR, Rahman M, Yu AC, Chan SK, Schaeffer DF, Kennecke HF, Lim HJ, Owen D, Tai IT. Nucleophosmin 1, upregulated in adenomas and cancers of the colon, inhibits p53-mediated cellular senescence. Int J Cancer 2013; 133: 1567-1577.

[18] Wang Z, Gall JM, Bonegio R, Havasi A, Illanes K, Schwartz JH, Borkan SC. Nucleophosmin, a Critical Bax Cofactor in Ischemia-Induced Cell Death. Mol Cell Biol 2013; 33: 1916-1924.

[19] Marasco D, Ruggiero A, Vascotto C, Poletto M, Scognamiglio PL, Tell G, Vitagliano L. Role of mutual interactions in the chemical and thermal stability of nucleophosmin NPM1 domains. Biochem Biophys Res Commun 2013; 430: 523-528.

[20] Pfister JA, D'Mello SR. insights into the regulation of neuronal viability by nucleophosmin/B23. Exp Biol Med (Maywood) 2015; 240: 774-786.

[21] Zhuravleva A, Radford SE. How TriC Folds Tricky Proteins. Cell 2014; 159: 1251-1252.

[22] Leitner A, Joachimiak LA, Bracher A, Mönkemeyer L, Walzthoeni T, Chen B, Pechmann S, Holmes S, Cong Y, Ma B, Ludtke S, Chiu W, Hartl FU, Aebersold R, Frydman J. The molecular architecture of the eukaryotic chaperonin TRiC/CCT. Structure 2012; 20: 814-825.

[23] Tracy CM, Gray AJ, Cuellar J, Shaw TS, Howlett AC, Taylor RM, Prince JT, Ahn NG, Valpuesta JM, Willardson BM. Programmed cell death protein 5 interacts with the cytosolic chaperonin containing tailless complex polypeptide 1 (CCT) to regulate β-tubulin folding. J Biol Chem 2014; 289: 4490-4502.

[24] Huang X, Wang X, Cheng C, Cai J, He S, Wang H, Liu F, Zhu C, Ding Z, Huang X, Zhang T, Zhang Y. Chaperonin containing TCP1, subunit 8 (CCT8) is upregulated in hepatocellular carcinoma and promotes HCC proliferation. APMIS 2014; 122: 1070-1079.
[25] Brackley KI, Grantham J. Activities of the chaperonin containing TCP-1 (CCT): implications for cell cycle progression and cytoskeletal organisation. Cell Stress Chaperones 2009; 14: 23-31.
[26] Esteves AR, Gozes I, Cardoso SM. The rescue of microtubule-dependent traffic recovers mitochondrial function in Parkinson's disease. Biochim Biophys Acta 2014; 1842: 7-21.
[27] Arduíno DM, Esteves AR, Cardoso SM. Mitochondria drive autophagy pathology via microtubule disassembly: a new hypothesis for Parkinson's disease. Autophagy 2012; 9: 112-4.
[28] Aridon P, Geraci F, Turturici G, D'Amelio M, Savettieri G, Sconzo G. Protective Role of Heat Shock Proteins in Parkinson's Disease. Neurodegener Dis 2011; 8: 155-168.
[29] Falsone SF, Kungl AJ, Rek A, Cappai R, Zangger K. The Molecular Chaperone Hsp90 Modulates Intermediate Steps of Amyloid Assembly of the Parkinson-related Proteinα-synuclein. J Biol Chem 2009; 284: 31190-31199.
[30] Daturpalli S, Wang S, Buell A, Waudby C, Meehan S, Jackson SE. Hsp90 Inhibits alpha-Synuclein Aggregation by Interacting with Soluble Oligomers. J Mol Biol 2013; 425: 4614-4628.
[31] Kiffin R, Christian C, Knecht E, Cuervo AM. Activation of chaperone mediated autophagy during oxidative stress. Mol Biol Cell 2004; 15: 4829-4840.
[32] Marin C, Aguilar E. In vivo 6-OHDA-induced neurodegeneration and nigral autophagic markers expression. Neurochem Int 2011; 58: 521-526.
[33] Uryu K, Richter-Landsberg C, Welch W, Sun E, Goldbaum O, Norris EH, Pham CT, Yazawa I, Hilburger K, Micsenyi M, Giasson BI, Bonini NM, Lee VM, Trojanowski JQ. Convergence of heat shock protein 90 with ubiquitin in filamentous alpha-synuclein inclusions of alpha-synucleinopathies. Am J Pathol 2006; 168: 947-961.
[34] Zhang L, Karsten P, Hamm S, Pogson JH, Lutz AK, Exner N, Haass C, Whitworth A, Winklhofer K, Schulz JB, Voigt A. TRAP1 rescues PINK1 loss-of-function phenotypes. Hum Mol Genet 2013; 22: 2829-2841.
[35] Hurtado-Lorenzo A, Anand VS. Heat Shock Protein 90 Modulates LRRK2 Stability: Potential Implications for Parkinson's Disease Treatment. J Neurosci 2008; 28: 6757-6759.
[36] Ou JR, Tan MS, Xie AM, Yu JT, Tan L. Heat Shock Protein 90 in Alzheimer's Disease. Biomed Res Int 2014; 2014: 796869.
[37] Shen HY, He JC, Wang Y, Huang QY, Chen JF. Geldanamycin induces heat shock protein 70 and protects against MPTP-induced dopaminergic neurotoxicity in mice. J Biol Chem 2005; 280: 39962-39969.
[38] Putcha P, Danzer KM, Kranich LR, Scott A, Silinski M, Mabbett S, Hicks CD, Veal JM, Steed PM, Hyman BT, McLean PJ. Brain-permeable small-molecule inhibitors of Hsp90 prevent alpha-synuclein oligomer formation and rescue alpha-synuclein-induced toxicity. J Pharmacol Exp Ther 2010; 332: 849-857.
[39] Luo W, Sun W, Taldone T, Rodina A, Chiosis G. Heat shock protein 90 in neurodegenerative diseases. Mol Neurodegener 2010; 5: 24.
[40] Kalia SK, Kalia LV, McLean PJ. Molecular Chaperones as Rational Drug Targets for Parkinson's Disease Therapeutics. CNS Neurol Disord Drug Targets 2010; 9: 741-753.
[41] McFarland NR, Dimant H, Kibuuka L, Ebrahimi-Fakhari D, Desjardins CA, Danzer KM, Danzer M, Fan Z, Schwarzschild MA, Hirst W, McLean PJ. Molecule Hsp90 Inhibitors Rescues Striatal Dopamine Levels but Not α-Synuclein-Induced Neuronal Cell Loss. PLoS One 2014; 9: e86048.
[42] Woodcock JM, Murphy J, Stomski FC, Berndt MC, Lopez AF. The dimeric versus monomeric status of 14-3-3zeta is controlled by phosphorylation of Ser58 at the dimer interface. J Biol Chem 2003; 278: 36323-36327.
[43] Toyo-Oka K, Wachi T, Hunt RF, Baraban SC, Taya S, Ramshaw H, Kaibuchi K, Schwarz QP, Lopez AF, Wynshaw-Boris A. 14-3-3ε and ζ Regulate Neurogenesis and Differentiation of Neuronal Progenitor Cells in the Developing Brain. J Neurosci 2014; 34: 12168-12181.
[44] Shirakashi Y, Kawamoto Y, Tomimoto H, Takahashi R, Ihara M. alpha-Synuclein is colocalized with 14-3-3 and synphilin-1 in A53T transgenic mice. Acta Neuropathol 2006; 112: 681-689.
[45] Slone SR, Lavalley N, McFerrin M, Wang B, Yacoubian TA. Increased 14-3-3 phosphorylation observed in Parkinson's disease reduces neuroprotective potential of 14-3-3 proteins. Neurobiol Dis 2015; 79: 1-13.
[46] Berg D, Holzmann C, Riess O. 14-3-3 proteins in the nervous system. Nat Rev Neurosci 2003; 4: 752-762.
[47] Wang J, Lou H, Pedersen CJ, Smith AD, Perez RG. 14-3-3zeta contributes to tyrosine hydroxylase activity in MN9D cells: localization of dopamine regulatory proteins to mitochondria. J Biol Chem 2009; 284: 14011-14019.
[48] Doggett EA, Zhao J, Mork CN, Hu D, Nichols RJ. Phosphorylation of LRRK2 serines 955 and 973 is disrupted by Parkinson's disease muta-

tions and LRRK2 pharmacological inhibition. J Neurochem 2012; 120: 37-45.
[49] Muda K, Bertinetti D, Gesellchen F, Hermann JS, von Zweydorf F, Geerlof A, Jacob A, Ueffing M, Gloeckner CJ, Herberg FW. Parkinson-related LRRK2 mutation R1441C/G/H impairs PKA phosphorylation of LRRK2 and disrupts its interaction with 14-3-3. Proc Natl Acad Sci U S A 2014; 111: E34-43.
[50] Sato S, Chiba T, Sakata E, Kato K, Mizuno Y, Hattori N, Tanaka K. 14-3-3eta is a novel regulator of parkin ubiquitin ligase. EMBO J 2006; 25: 211-221.
[51] Halskau O, Ying M, Baumann A, Kleppe R, Larrea DR, Almaas B, Haavik J, Martinez A. Threeway interaction between 14-3-3 proteins, the N-terminal region of tyrosine hydroxylase, and negatively charged membranes. J Biol Chem 2009; 284: 32758-32769.
[52] Kurz A, May C, Schmidt O, Müller T, Stephan C, Meyer HE, Gispert S, Auburger G, Marcus K. A53T -alpha-synuclein-overexpression in the mouse nigrostriatal pathway leads to early increase of 14-3-3 epsilon and late increase of GFAP. J Neural Transm 2012; 119: 297-312.
[53] Yacoubian TA, Slone SR, Harrington AJ, Hamamichi S, Schieltz JM, Caldwell KA, Caldwell GA, Standaert DG. Differential neuroprotective effects of 14-3-3 proteins in models of Parkinson's disease. Cell Death Dis 2010; 1: e2.
[54] Slone SR, Lesort M, Yacoubian TA. 14-3-3theta protects against neurotoxicity in a cellular Parkinson's disease model through inhibition of the apoptotic factor Bax. PLoS One 2011; 6: e21720.
[55] Porter GW, Khuri FR, Fu H. Dynamic 14-3-3/client protein interactions integrate survival and apoptotic pathways. Semin Cancer Biol 2006; 16: 193-202.
[56] Xing H, Zhang S, Weinheimer C, Kovacs A, Muslin AJ. 14-3-3 proteins block apoptosis and differentially regulate MAPK cascades. EMBO J 2000; 19: 349-358.
[57] Subramanian RR, Zhang H, Wang H, Ichijo H, Miyashita T, Fu H. Interaction of apoptosis signal-regulating kinase 1 with isoforms of 14-3-3 proteins. Exp Cell Res 2004; 294: 581-591.
[58] Yang H, Masters SC, Wang H, Fu H. The proapoptotic protein Bad binds the amphipathic groove of 14-3-3zeta. Biochim Biophys Acta 2001; 1547: 313-319.
[59] Chen XW, Sun SG, Cheng DB, Tian YY. Overexpression of 14-3-3 protein protects pheochromocytoma cells against 1-methyl-4-phenylpyridinium toxicity. Neurosci Bull 2006; 22: 281-287.
[60] Nomura M, Shimizu S, Sugiyama T, Narita M, Ito T, Matsuda H, Tsujimoto Y. 14-3-3 Interacts directly with and negatively regulates pro-apoptotic Bax. J Biol Chem 2003; 278: 2058-2065.
[61] Nutt LK, Buchakjian MR, Gan E, Darbandi R, Yoon SY, Wu JQ, Miyamoto YJ, Gibbon JA, Andersen JL, Freel CD, Tang W, He C, Kurokawa M, Wang Y, Margolis SS, Fissore RA, Kornbluth S. Metabolic control of oocyte apoptosis mediated by 14-3-3zeta-regulated dephosphorylation of caspase-2. Dev Cell 2009; 16: 856-866.
[62] Brunet A, Bonni A, Zigmond MJ, Lin MZ, Juo P, Hu LS, Anderson MJ, Arden KC, Blenis J, Greenberg ME. Akt promotes cell survival by phosphorylating and inhibiting a Forkhead transcription factor. Cell 1999; 96: 857-868.
[63] Linde CI, Di Leva F, Domi T, Tosatto SC, Brini M, Carafoli E. Inhibitory interaction of the 14-3-3 proteins with ubiquitous (PMCA1) and tissue-specific (PMCA3) isoforms of the plasma membrane Ca2+ pump. Cell Calcium 2008; 43: 550-561.